were obtained by slow evaporation of an ether/*n*-hexane solution (mp 151-152 °C)); $^1$H NMR (250 MHz, $CD_2Cl_2$) $\delta$ 7.30 ppm (m, 2 H), 6.85 ppm (m, 3 H), 4.51 ppm (br s, 2 H), 2.86 ppm (dd, $J \approx 15.2$ Hz, $J \approx 1$ Hz, 2 H), 2.73 ppm (dd, $J \approx 15.2$ Hz, $J \approx 3.3$ Hz, 2 H), 2.14 ppm (m, 2 H), 1.69 ppm (dd, $J \approx 14.6$ Hz, $J \approx 6.8$ Hz, 2 H); IR ($CHCl_3$) 3030 (w), 2960 (m), 2880 (w), 2230 (s), 1590 (s), 1495 (s) cm$^{-1}$.

***N*-Phenyl-4-azacyclohexylidenemalononitrile (4)** was synthesized by stirring and refluxing under nitrogen a mixture of **8** (1.60 g, 9.1 mmol), malononitrile (0.59 g, 8.9 mmol), 0.67 g of ammonium acetate, and 1.5 mL of acetic acid in ca. 50 mL of benzene for 1.5 h in a Dean-Stark apparatus. After cooling, the clear light orange reaction mixture was washed with water, saturated sodium bicarbonate, and water. The combined organic solutions were dried ($MgSO_4$), filtrated, and evaporated to dryness. The yellow solid was recrystallized from ethyl acetate: yield 60%; dec ca. 139 °C (suitable crystals for X-ray analysis were obtained by slow evaporation of an ether/$CH_2Cl_2$ solution); $^1$H NMR (250 MHz, $CD_2Cl_2$) $\delta$ 7.28 ppm (m, 2 H), 6.91 ppm (m, 3 H), 3.48 ppm (t, $J \approx 6$ Hz, 4 H), 2.84 ppm (t, $J \approx 6$ Hz, 4 H); IR ($CHCl_3$) 3050 (w), 3020 (w), 2970 (w), 2830 (w), 2230 (s), 1600 (s), 1500 (s) cm$^{-1}$; high-resolution MS found $m/z$ 223.1092, calcd for $C_{14}H_{13}N_3$ $m/z$ 223.1074.

***N*-(*p*-Methoxyphenyl)-8-azabicyclo[3.2.1]octylidene-3-malononitrile (5)** could be synthesized by stirring and refluxing a mixture of the ketone **10** (216.9 mg, 0.94 mmol), malononitrile (74.5 mg, 1.13 mmol), 222 mg of ammonium acetate, and 0.2 mL of acetic acid in ca. 5 mL of benzene for 2.25 h in a Dean-Stark apparatus (filled with molsieves 4Å). The same workup as described for **3** yielded a yellow solid which was recrystallized from ether/$CH_2Cl_2$: yield 53%; Mp 200 °C (suitable crystals for X-ray analysis were obtained by slow evaporation of an ether/$CH_2Cl_2$ (1:1) solution; mp 202 °C); $^1$H NMR (200 MHz, $CDCl_3$) $\delta$ 6.86 ppm (m, 4 H), 4.44 ppm (br s, 2 H), 3.78 ppm (s, 3 H), 2.84 ppm (d with fine coupling, $J \approx 14$ Hz, 2 H), 2.75 ppm (d with fine coupling, $J \approx 14$ Hz, 2 H), 2.16 ppm (m, 2 H), 1.68 ppm (m, 2 H); IR ($CHCl_3$) 3030 (w), 2960 (m), 2225 (m), 1580 (m), 1510 (s) cm$^{-1}$; high-resolution MS found $m/z$ 279.1355, calcd for $C_{17}H_{17}N_3O$ $m/z$ 279.1372.

***N*-(*p*-Methoxyphenyl)-4-azacyclohexylidenemalononitrile (6)** was prepared by stirring and refluxing the ketone **11** (146.9 mg, 0.72 mmol), malononitrile (73.1 mg, 1.11 mmol), 150 mg of ammonium acetate, and 0.11 mL of acetic acid in 3 mL of toluene for 2.5 h in a Dean-Stark apparatus. After the usual workup, a red oil, which became solid in the refrigerator, was isolated. Recrystallization from $CH_2Cl_2$/ether (1:1) yielded red crystals. Further purification by flash column chromatography (Merck kieselgel 60 (0.04-0.063 mm), PE/ether (1:3) as eluens) yielded a yellow crystalline compound: yield 76%; mp 129-130 °C (suitable crystals for X-ray analysis were obtained by slow evaporation of an ether/$CH_2Cl_2$ solution); $^1$H NMR (250 MHz, $CDCl_3$) $\delta$ 6.87 ppm (m, 4 H), 3.77 ppm (s, 3 H), 3.34 ppm (t, $J \approx 5.6$ Hz, 4 H), 2.86 ppm (t, $J \approx 5.6$ Hz, 4 H); IR ($CHCl_3$) 3000 (m), 2960 (m), 2930 (m), 2905 (m), 2830 (m), 2230 (m), 1595 (m), 1510 (s) cm$^{-1}$.

**Acknowledgment.** The present investigations were supported in part by the Netherlands Organization for Chemical Research (SON) with financial aid from the Netherlands Organization for the Advancement of Research (NWO). For the MM2P calculations and CSD searches use of the services and facilities of the Dutch CAOS/CAMM Center under Grant Nos. SON-11-20-700 and STW-NCH-44.0703 is gratefully acknowledged.

**Supplementary Material Available:** Tables (S1 and S2) giving the crystallographic data, the final coordinates, and equivalent thermal parameters for compounds **3-6** (4 pages). Ordering information is given on any current masthead page.

# Nature of Coenzyme Binding by Glyceraldehyde-3-phosphate Dehydrogenase: $^{13}$C NMR Studies with Oxidized [4-$^{13}$C]Nicotinamide Adenine Dinucleotide†

**Jürgen Klepp,‡ Margit Oberfrank,‡ János Rétey,*‡ Denis Tritsch,§ Jean-François Biellmann,*§ and William E. Hull*‖**

*Contribution from the Lehrstuhl für Biochemie, Institut für Organische Chemie der Universität Karlsruhe, D-7500 Karlsruhe, West Germany, the Laboratoire de Chimie Organique Biologique, Institut de Chimie, Université Louis Pasteur, F-67008 Strasbourg, France, and the Central Department of Spectroscopy, German Cancer Research Center, D-6900 Heidelberg, West Germany.* *Received March 31, 1988*

**Abstract:** The tetrameric enzyme glyceraldehyde-3-phosphate dehydrogenase from sturgeon muscle is known to exhibit negative cooperativity of NAD binding, with the first two coenzyme molecules being bound much tighter than the third and fourth molecules. We have examined the binding process directly using 125-MHz $^{13}$C NMR spectroscopy by titrating the apoenzyme (ca. 170 $\mu$M) at 15 °C with the labeled coenzyme [4-$^{13}$C]NAD. At a stoichiometry of 2 NAD/tetramer virtually all the coenzyme is bound, but only the hint of a broad signal for the bound $\beta$-[4-$^{13}$C]NAD could be seen. At 4 NAD/tetramer a strong signal for bound NAD ($\delta_c$ = 153 ppm, $\Delta\nu$ = 260 Hz) was detected, but it integrated to just 2 equiv/tetramer, while the other two NAD remained "invisible". With 5-6 NAD/tetramer the expected amount of free NAD was detected ($\delta_c$ = 146.95 ppm), and the integral of the bound NAD signal also increased to show four equivalent NAD molecules bound. This behavior requires a model in which the first two NAD bind tightly, but in a complex which exhibits an intermediate rate of exchange between two bound forms, E·NAD and E′·NAD, with different NAD chemical shifts, leading to coalescence broadening ($\Delta\nu > 500$ Hz). Binding of the third NAD results in the stabilization of the E′·NAD conformation for one subunit and the appearance of a detectable signal for bound NAD. Binding of the fourth NAD leads to a cooperative transition to give the symmetrical holoenzyme with four E′·NAD subunits. The driving force for this E → E′ conversion is provided at the expense of the binding energy of the third and fourth NAD (negative cooperativity). Analysis of the $^{13}$C NMR line-width behavior of free NAD yields the apparent dissociation rate constant for NAD from the holoenzyme, $k_{-1}^{app}$ = 23 s$^{-1}$ at 15 °C. The 6 ppm downfield shift of C-4 for bound vs free NAD rules out mechanistic models involving nucleophilic addition at C-4 of Cys$^{149}$, for example.

Glyceraldehyde-3-phosphate dehydrogenase from various sources is a tetramer with MW ~ 145 000. The subunits are identical in their amino acid sequence,[1] and no differences between the individual polypeptide chains could be detected with respect to their conformation as determined by X-ray diffraction at 2.4-3.0-Å resolution.[2] Kinetic and equilibrium studies revealed, however, that the enzyme isolated for instance from sturgeon muscle,[3] from *Bacillus stearothermophilus*,[4] from rabbit muscle,[4-6]

† Dedicated to Professor Duilio Arigoni on the occasion of his 60th birthday.
‡ Institut für Organische Chemie der Universität Karlsruhe.
§ Institut de Chemie.
‖ German Cancer Research Center.

(1) Jones, G. M. T.; Harris, J. J. *FEBS Lett.* **1972**, *22*, 185-189.
(2) Leslie, A. G. W.; Wonacott, A. J. *J. Mol. Biol.* **1984**, *178*, 743-772, and references cited therein.

0002-7863/89/1511-4440$01.50/0 

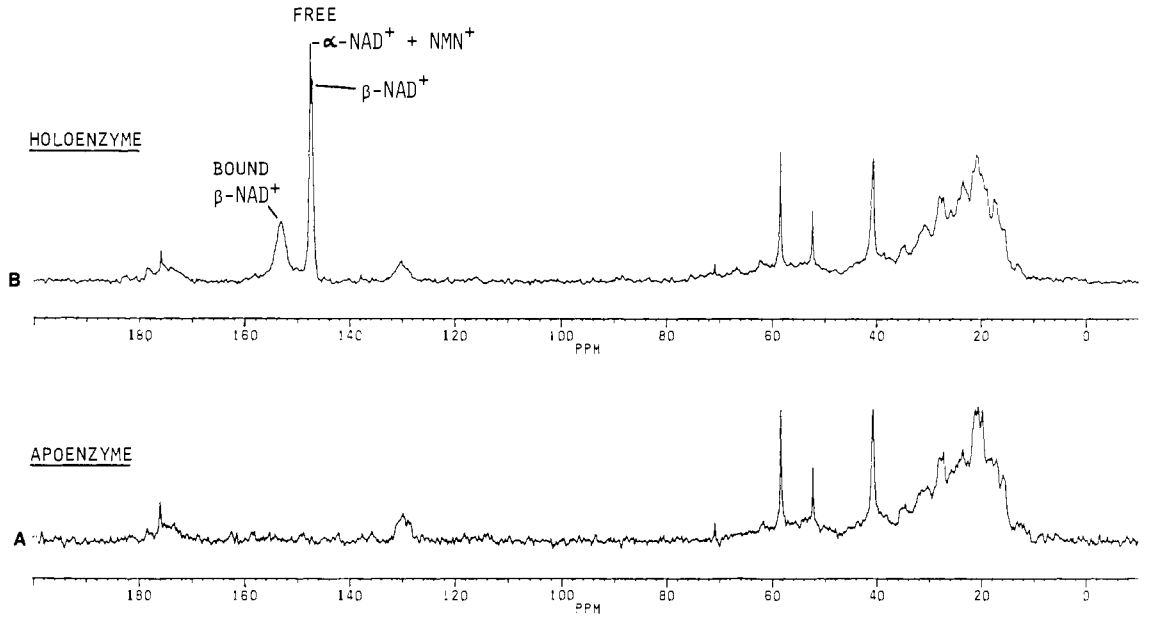


**Figure 1.** 125.7-MHz $^{13}C$ NMR spectra at 15 °C of ca. 170 μM apo-glyceraldehyde-3-phosphate dehydrogenase (A) and the holoenzyme (B) generated by adding an excess (5.62 β-NAD/tetramer) of [4-$^{13}C$]NAD. The inverse-gated $^{1}H$-decoupled spectra required 5000 and 20000 transients, respectively. Sharp peaks at 52, 59, 71, and 176 ppm are from buffer solution.

**Table I.** $^{13}C$ NMR Data for the Titration of Tetrameric Apo-GAPDH with [4-$^{13}C$]NAD$^+$

| | | $^{13}C$ NMR chemical shifts and integrals[c] | | | | | |
|---|---|---|---|---|---|---|---|
| spectrum no.[a] | total β-NAD$^+$/ tetramer ratio[b] | β-NAD$^+$ bound (153 ppm) | β-NAD$^+$ free (146.95 ppm) | α-NAD$^+$ (147.32 ppm) | NMN$^+$ (147.62 ppm) | total β-NAD$^+$ observed | total β-NAD$^+$ expected[d] |
| 1.1 | 0 | <5.0 | | | | | |
| 1.2 | 0.68 | <10.0 | | 2.0 | | <10.0 | 10.6 |
| 1.3 | 1.37 | 11.8 | 1.0 | 4.6 | 1.2 | 12.8 | 24.2 |
| 1.4 | 2.06 | 16.3 | 1.5 | 6.9 | 1.8 | 17.8 | 36.3 |
| 2.2 | 2.08 | 24.9 | 1.2 | 10.2 | 6.5 | 26.1 | 45.3 |
| 2.3 | 2.72 | 32.9 | 1.9 | 12.9 | 8.0 | 34.8 | 57.3 |
| 1.5 | 2.76 | 14.0 | 1.5 | 9.6 | 2.1 | 15.5 | 50.5 |
| 2.4 | 3.25 | 28.8 | 1.9 | 14.3 | 10.9 | 30.7 | 63.6 |
| 2.5 | 3.98 | 36.6 | 3.3 | 21.1 | 12.8 | 39.9 | 93.8 |
| 1.6 | 4.18 | 43.3 | 4.4 | 16.2 | 3.4 | 47.7 | 85.3 |
| 1.7 | 5.62 | 72.7 | 29.3 | 20.7 | 4.9 | 102.0 | 108.9 |
| 1.7b | 5.62 | 75.2 | 29.9 | 21.2 | 5.5 | 105.1 | 111.6 |
| 1.8 | 6.71 | 90.0 | 45.4 | 24.6 | 6.3 | 135.4 | 129.5 |
| 1.9 | 8.14 | 94.0 | 75.0 | 28.7 | 7.1 | 169.0 | 151.1 |
| 1.9b | 8.14 | 86.0 | 75.2 | 28.8 | 7.0 | 161.0 | 151.6 |

[a] Numbering is as in Table II and the figures; [GAPDH] = ca. 170 μM (series 1) or ca. 120 μM (series 2); some of the data are plotted in Figure 4. [b] Based on YADH assay (Table II). [c] Integrals from the individual spectra after an absolute-intensity Fourier transform are in arbitrary units and have been scaled to account for the number of transients acquired and the enzyme concentration (see Experimental Section); precision is estimated to be ±5 for bound β-NAD$^+$ and ±1 for free species. [d] Based on the integral for α-NAD$^+$ and the composition of the coenzyme reagent (Table II).

and from lobster muscle[7] exhibits negative cooperativity in the binding of NAD$^+$. In general, the first two binding sites could not be distinguished and feature very tight binding with $K_D < 0.5$ μM. Binding to the third and fourth sites was found to be progressively weaker with $K_D$ values ranging from 0.5 to 10 μM, depending on enzyme and methods. Two different models have been proposed to account for this behavior. The induced-fit model explains negative cooperativity as the result of conformational changes induced by the initial binding of NAD$^+$.[8] The preexistent asymmetry model postulates a tetramer configuration in which the NAD$^+$ affinity of two subunits differs markedly from that of the others, in spite of the identical conformation for all four subunits when they are dissociated.[9] We report here on the use of [4-$^{13}C$]NAD$^+$[10] for elucidating the nature of NAD$^+$ binding to sturgeon muscle glyceraldehyde-3-phosphate dehydrogenase (GAPDH). The NAD$^+$-free apoenzyme from this source can be easily prepared and is stable.[3,11]

## Results

GAPDH from sturgeon muscle was isolated according to an established procedure.[3] Unless otherwise stated NMR experiments were carried out at 15 °C, where the enzyme showed good stability. Two independent series of experiments utilized different enzyme and coenzyme preparations. The data in the tables and figures are given the notations 1.*n* or 2.*n*, referring to the *n*th experiment in series 1 or 2, respectively. The natural abundance $^{13}C$ NMR spectrum of the coenzyme-free apoform of GAPDH is virtually devoid of signals in the range between 135 and 160

(3) Seydoux, F.; Bernhard, S.; Pfenninger, O.; Payne, M.; Malhotra, O. P. *Biochemistry* **1973**, *12*, 4290–4300.
(4) Allen, G.; Harris, J. J. *Biochem. J.* **1975**, *151*, 747–759.
(5) Conway, A.; Koshland, D. E., Jr. *Biochemistry* **1968**, *7*, 4011–4023.
(6) Boers, W.; Osthüizen, C.; Slater, E. C. *Biochim. Biophys. Acta* **1971**, *250*, 35–46.
(7) De Vijlder, J. J. M.; Boers, W.; Slater, E. C. *Biochim. Biophys. Acta* **1969**, *191*, 214–220.
(8) Koshland, D. E., Jr.; Némethy, G.; Filmer, D. *Biochemistry* **1966**, *5*, 365–385.
(9) Malhotra, O. P.; Bernhard, S. A. *J. Biol. Chem.* **1968**, *243*, 1243–1252.
(10) Oberfrank, M.; Hull, W. E.; Rétey, J. *Eur. J. Biochem.* **1984**, *140*, 157–161.
(11) Branlant, G.; Eiler, B.; Biellmann, J. F.; Lutz, H. P.; Luisi, P. L. *Biochemistry* **1983**, *22*, 4437–4443.

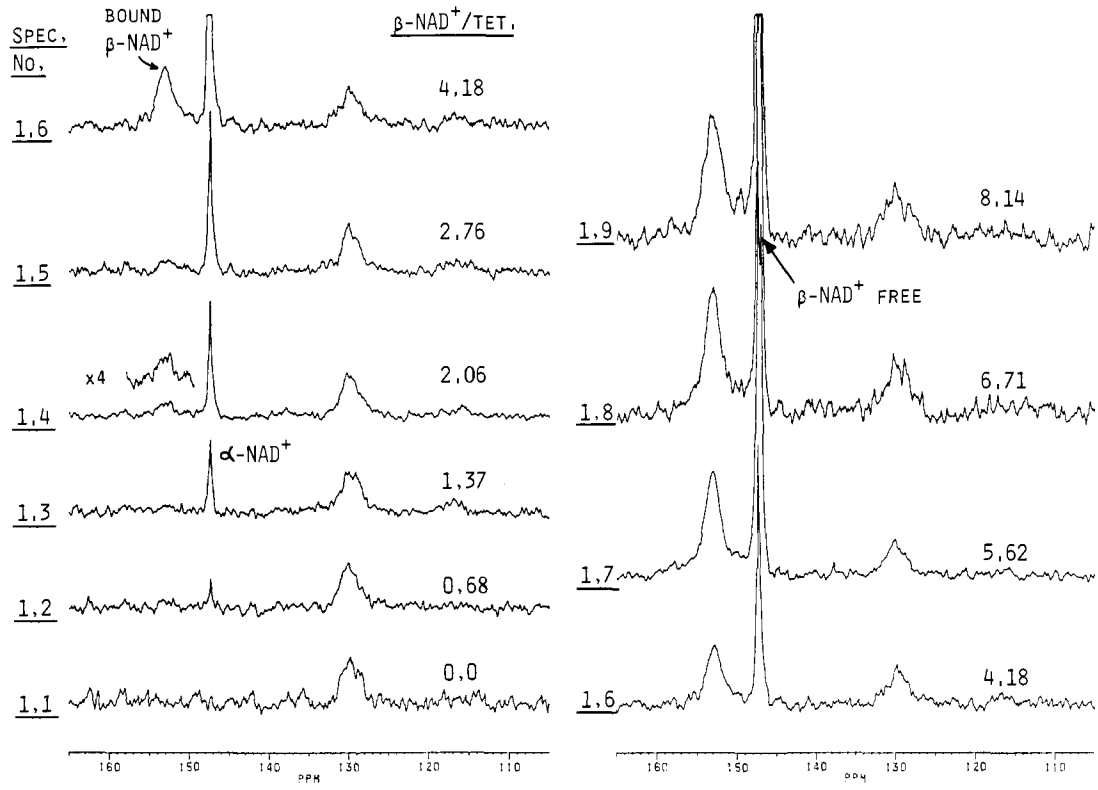


**Figure 2.** Aromatic signal region of the 125.7-MHz $^{13}C$ NMR spectra (series 1, Table I) for the titration of GAPDH with [4-$^{13}C$]NAD. The spectra are labeled according to Table I with the ratio of total β-NAD/tetramer and are plotted after scaling to give correct relative signal intensities. The differing noise levels are thus a result of the differing number of transients acquired.

ppm (Figure 1A), where the signal for the $^{13}C$-4 atom of the nicotinamide ring appears at $\delta_c$ = 153 ppm when the holoenzyme is prepared with [4-$^{13}C$]$NAD^+$ (Figure 1B). Stepwise addition of completely (99%) and specifically labeled [4-$^{13}C$]$NAD^+$ caused initially little change in the $^{13}C$ NMR spectrum (Figure 2, spectra 1.2 and 1.3), except for the immediate appearance and proportional increase of the signals for α-[4-$^{13}C$]$NAD^+$ ($\delta_c$ = 147.32 ppm) and [4-$^{13}C$]$NMN^+$ ($\delta_c$ = 147.62 ppm), which were present as contaminants in the coenzyme solution (Table I, legend to Table II). These species and free β-$NAD^+$ could be resolved and quantitated in resolution-enhanced spectra (Figure 3). Since their chemical shifts and line widths were independent of concentration and were the same in the absence of enzyme, α-$NAD^+$ and $NMN^+$ do not interact with the enzyme, and quantitation of their signals serves as an internal check and calibration for the total amount of β-$NAD^+$ added during the titration. The interaction of β-NAD (the notation [4-$^{13}C$] and the (+) sign will be hereafter omitted) with apoenzyme was apparent in that, in the initial phase of the titration, very little signal appeared at $\delta_c$ = 146.95 ± 0.05 ppm, the position for free β-NAD in the absence of enzyme (Figure 2, Table I). Surprisingly, the expected signal for the presumably tightly bound β-NAD could not be detected either. When the integral over the region 149–156 ppm was computed, only about half of the expected value (based on the amount of β-NAD titrated) was obtained (Table I, Figure 4). At 2–3 β-NAD/tetramer a weak broad resonance at $\delta_c$ = 153 ppm could be detected, but its integral was still significantly less than the value expected for the amount of β-NAD added (spectra 1.4 and 1.5). When 4 equiv of β-NAD/tetramer had been added (Figures 2 and 3, spectrum 1.6), the broad signal for bound coenzyme, centered at $\delta_c$ = 153 ppm, could be clearly distinguished, but its integral represented within experimental error just half the amount of β-NAD added. Further addition of coenzyme to give 5.6 equiv of β-NAD/tetramer (spectrum 1.7) resulted simultaneously in nearly equal increases in the bound coenzyme signal and the signal of free β-NAD (Figures 3 and 4). *At this point the total amounts of β-NAD observed and expected were in agreement.* The amount of bound coenzyme reached a maximum at 6–7 β-NAD/tetramer.

A plot of the signal integral for free coenzyme vs the ratio of added coenzyme/tetramer (Figure 4) shows quite accurately that four molecules of β-NAD are tightly bound per enzyme tetramer. At 2–4 β-NAD/tetramer a small amount of free β-NAD could be detected (resolution-enhanced spectra) in slow exchange with bound coenzyme, and when excess β-NAD was added, the expected linear increase in free β-NAD was observed. The accuracy of the titration stoichiometries and the precision of the NMR analysis can be judged by the linear behavior of the data for the noninteracting species α-NAD.

The nonlinear behavior of the signal for bound β-NAD as the enzyme is titrated with coenzyme could also be visualized in the $^{13}C$ NMR difference spectra (not shown) computed for successive addition of aliquots of the coenzyme solution. Initially, for equal aliquots of β-NAD up to 2.76 equiv/tetramer, only the nonbinding species α-NAD and NMN exhibit equal signal increments. Detectable increments in the broad signal for bound coenzyme at 153 ppm are observed only when the β-NAD/tetramer ratio is raised from 2.76 to 4.18 and from 4.18 to 5.62. Further titration results in little further change in bound coenzyme but gives the expected increments in free β-NAD, α-NAD, and NMN.

Evidence for a substantial change in protein conformation upon NAD binding is provided by the aliphatic signal region of the difference spectra (Figure 5). Small changes in the chemical shifts of various side-chain signals can be detected with the addition of each aliquot of coenzyme, but the effects are best seen by comparing spectra with 0, 2.76, 5.62, and 6.71 equiv of coenzyme. A major effect has already occurred at half-saturation with coenzyme. Further but different changes appear to take place at saturation when all bound NAD becomes detectable. The necessarily poor signal/noise ratio in the natural abundance spectra of the enzyme does not allow more than these qualitative conclusions.

The possibility that initially bound β-NAD is "missing" because of conversion to NADH can be ruled out by several arguments. First, the presence of the substrate glyceraldehyde 3-phosphate in our apoenzyme preparations is unlikely since no NADH formation was detected by fluorescence measurements without ad-

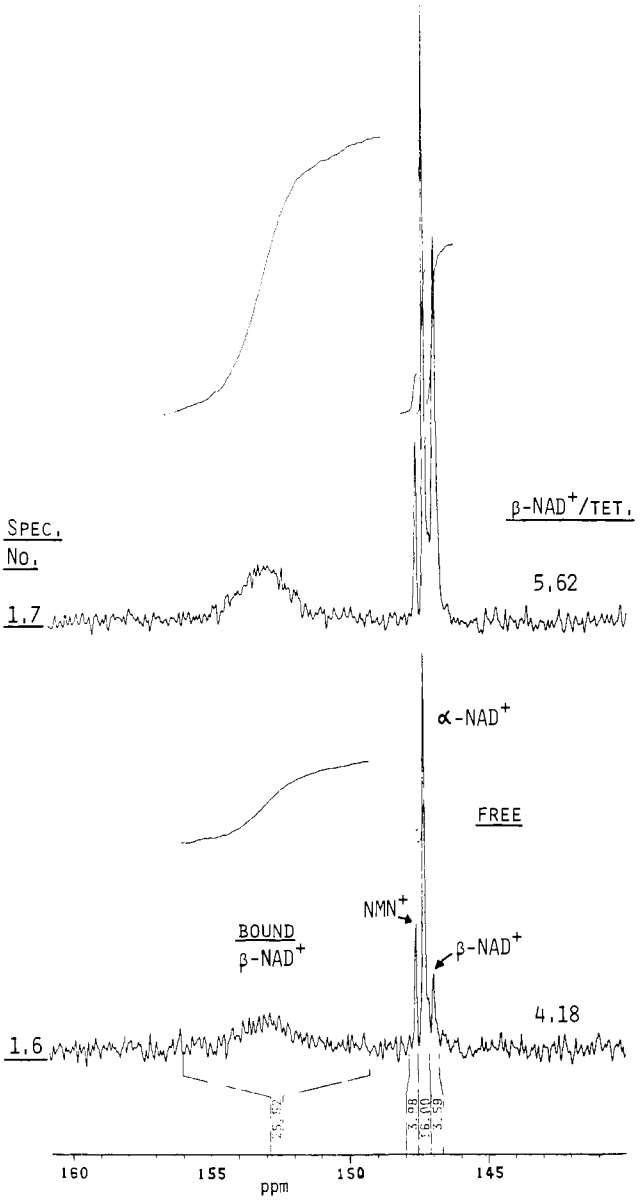


**Figure 3.** Resolution-enhanced 125.7-MHz $^{13}C$ NMR spectra of GAPDH/NAD samples 1.6 and 1.7 (Table I) showing the resolution and integration of all free and bound [4-$^{13}C$]nicotinamide species.

**Scheme I**

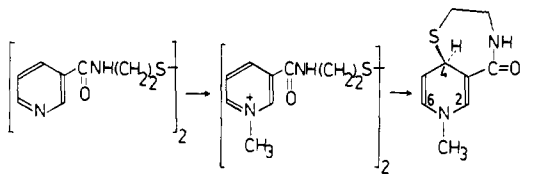

1 2 3

dition of substrate.[11] Also the Racker band,[12] which is believed to arise from the interaction of NAD with the apoenzyme, shows initially a linear increase upon addition of NAD to the sturgeon enzyme prepared in the same way as in our case.[3,13] Second, the $^{13}C$ NMR difference spectra (Figure 5) do not show any substantial net positive signal at ca. 23 ppm where [4-$^{13}C$]NADH should appear. Most convincingly, in the presence of excess β-NAD the total integral for bound and free β-NAD corresponds, within experimental error (±5%), to the amount expected on the basis of the α-NAD integral (Table I).

(12) Racker, E.; Krimsky, I. *J. Biol. Chem.* **1952**, *198*, 731–743.
(13) Kelemen, N.; Kellershohn, N.; Seydoux, F. *Eur. J. Biochem.* **1975**, *57*, 69–78.

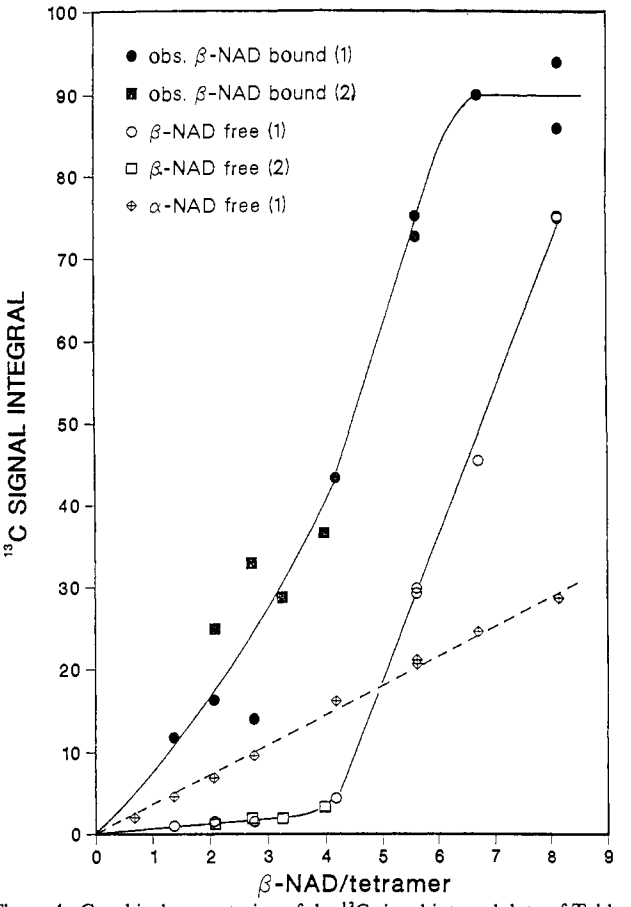


**Figure 4.** Graphical presentation of the $^{13}C$ signal integral data of Table I (observed β-NAD bound and free for series 1 and 2, α-NAD for series 1) are plotted vs the ratio of total β-NAD/tetramer. The data for α-NAD, which does not bind to GAPDH, demonstrate the linearity and precision of the NMR analysis. The data for free β-NAD show a tight binding stoichiometry of four coenzyme molecules per tetramer. The data for bound β-NAD show a sigmoidal behavior, indicating that below full saturation a significant portion of the bound coenzyme cannot be detected.

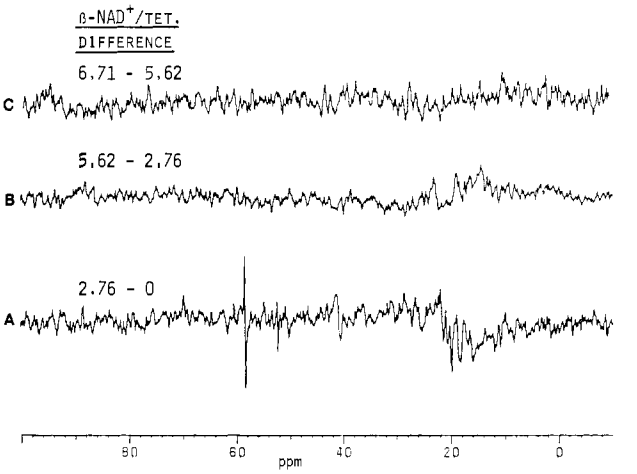


**Figure 5.** $^{13}C$ NMR difference spectra (aliphatic signal region) for GAPDH titrated with [4-$^{13}C$]NAD. (A) The addition of 2.76 equiv of β-NAD to the tetramer results in substantial changes in the amino acid side-chain resonances, indicative of large-scale effects on the protein. (B) Further but apparently different conformational changes occur when the third and fourth coenzyme molecules are bound. (C) After all four bound β-NAD become detectable (5.62 β-NAD/tetramer, spectrum 1.7 in Figure 2), no further conformational changes are detected with addition of coenzyme.

The hypothesis that nucleophilic addition of sulfur via a cysteine residue may occur at C-4 of bound β-NAD could also be tested

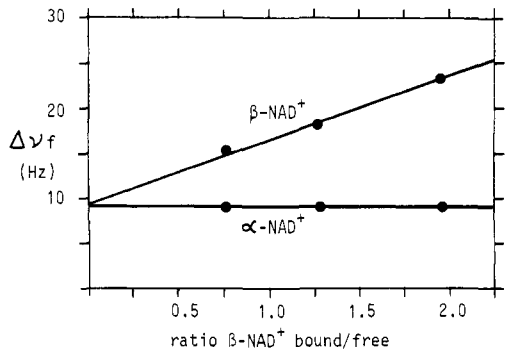


Figure 6. Plot of the $^{13}C$ NMR signal line width $\Delta\nu_f$ for free NAD vs the ratio of bound/free $\beta$-NAD (see eq 3), demonstrating the slow-exchange binding behavior of $\beta$-NAD with GAPDH and the absence of binding for $\alpha$-NAD. The residual line width in the absence of exchange ($\Delta\nu_o$ = 9 Hz) is limited by the digital resolution and data processing parameters chosen.

by $^{13}C$ NMR. We prepared a model compound (**3**, see Scheme I and Experimental Section) which carried a sulfur ligand at an $sp^3$-hybridized C-4. The $^{13}C$ NMR signal at $\delta_c$ = 70.09 ppm could be assigned to C-4, while C-2, C-5, and C-6 gave signals at 143.44, 120.1, and 139.66 ppm, respectively (in $CD_3OD$). The spectrum of Figure 1B and the difference spectra of Figure 5 show no evidence of a signal in the vicinity of 70 ppm at any stage of the titration.

The line width and chemical shift of the signal for bound $\beta$-NAD show no dependence on stoichiometry for 2.7–8 $\beta$-NAD/tetramer. For the saturated holoenzyme the bound $\beta$-NAD line width was 260 ± 30, 210 ± 20, and 300 ± 20 Hz at 15, 23, and 30 °C, respectively.

Further information concerning the kinetics of NAD binding can be obtained by examining the behavior of the line width of the free NAD species as excess coenzyme is added. In Figure 6 the line widths $\Delta\nu_f$ at 15 °C for free $\alpha$- and $\beta$-NAD are plotted vs the ratio of bound/free coenzyme. The line width for $\alpha$-NAD is constant, confirming that it does not interact with the enzyme. The line width for free $\beta$-NAD increases linearly (without a measurable change in chemical shift) with the ratio bound/free. This is indicative of chemical exchange in the slow-exchange limit, and the slope of the line defines a dissociation rate constant for $\beta$-NAD (Discussion).

## Discussion

**Three-Site Exchange Model for $\beta$-NAD Binding.** If $\beta$-NAD binding to each subunit of GAPDH involved simply independent two-site exchange between free and bound forms, then two possible results for the titration experiment are predicted. In the slow-exchange tight-binding case (enzyme concentration $\gg K_D$) bound $\beta$-NAD should appear at the beginning of the titration and increase essentially linearly until saturation is achieved, at which point free $\beta$-NAD will begin to appear. The line width of bound $\beta$-NAD will be largely insensitive to the ratio $\beta$-NAD/tetramer and will be determined by the sum of the natural bound line width and the kinetic contribution $k_{-1}/\pi$ for the dissociation rate. When $\beta$-NAD is in slight excess, its line width will be broadened proportional to $k_{-1}$ and will decrease as $\beta$-NAD is added. However, the behavior of GAPDH agrees with a two-site slow-exchange model only at $\beta$-NAD/tetramer > 4.

In the intermediate- to fast-exchange case only a single exchange-averaged resonance for bound and free $\beta$-NAD will be observed with line width and chemical shift depending on the fraction bound. In a previous study[10] of the binding of NAD to yeast alcohol dehydrogenase (YADH), only a single exchanged-averaged resonance for free and bound $\beta$-NAD was observed with a downfield shift for C-4 (compared to free $\beta$-NAD in the absence of enzyme) of ca. 1.7 ppm for 0.6 NAD/binding site.

For intermediate exchange rates approaching coalescence, the signal may become too broad to detect, with an additional linewidth contribution proportional to the difference in chemical shifts. The failure to detect by NMR most of the bound coenzyme at a stoichiometry of 0–2 $\beta$-NAD/tetramer and half the coenzyme at 2–4 $\beta$-NAD/tetramer *must* be the result of chemical exchange effects in the intermediate or coalescence regime. However, the fact that below saturation of enzyme sites a small amount of free $\beta$-NAD can be observed (Figure 4) with little exchange line width requires that exchange between free and bound coenzyme must be very slow, even when bound $\beta$-NAD is "invisible". Slow exchange is also implicated by the classical binding data in the literature.[3]

The apparently conflicting results obtained for GAPDH can be resolved by a three-site model in which a conformational equilibrium occurs after formation of the initial Michaelis complex (eq 1), where E represents a monomer subunit of GAPDH, E·

$$E + NAD \underset{k_{-1}}{\overset{k_1}{\rightleftharpoons}} E{\cdot}NAD \underset{k_{-2}}{\overset{k_2}{\rightleftharpoons}} E'{\cdot}NAD \qquad (1)$$

NAD is an initial complex ($K_D = k_{-1}/k_1$) with some change in NAD chemical shift, and E′·NAD is the final complex ($K_2 = k_2/k_{-2}$) with further alterations at the binding site that result in the large downfield shift for detected bound $\beta$-NAD. This scheme allows for slow exchange with respect to NAD and E·NAD but provides for the possibility of intermediate exchange broadening of bound $\beta$-NAD in the second step. It also provides a mechanism in which subunit interaction can influence the NMR signal for bound $\beta$-NAD via effects on $k_2$ and $k_{-2}$. In this model the notations E and E′ refer to the state of the subunit in the direct vicinity of the nicotinamide ring as monitored by C-4. The initial binding of $\beta$-NAD leads of course to a significant perturbation of the enzyme's $^{13}C$ spectrum as depicted in the difference spectra (Figure 5), even before the specific conversion from E to E′ takes place.

For the case of exchange between two equally populated sites with resonance frequencies (in Hz) of $\nu_A$ and $\nu_B$, coalescence occurs when the lifetime in either site $\tau_{ex} \approx 0.45/(\nu_A - \nu_B)$. Under these conditions the additional contribution to the line width of the coalesced signal will be ca. $\nu_A - \nu_B$.[14] If we assume that the chemical shift difference for C-4 in E·NAD and E′·NAD is 3–6 ppm, then coalescence can occur for $k_2 \sim k_{-2} \sim 1/\tau_{ex} \sim 10^3\ s^{-1}$. The coalesced signal will then have a line width $\Delta\nu_b > 500$ Hz and be difficult to detect under our conditions. If the equilibrium favors E′·NAD ($K_2 \gg 1$), then the maximum broadening at coalescence is reduced to $(1 - p)(\nu_A - \nu_B)$, where $p$ is the fractional population of the E′ state. In the slow-exchange limit the kinetic line-width contribution for E′·NAD becomes $pk_{-2}/\pi$. Thus, the appearance of the bound species E′·NAD only at $\beta$-NAD/tetramer > 2 indicates that *initially the conformational equilibrium (step 2 in eq 1) for the first two binding sites is in the coalescence regime* with comparable populations of E·NAD and E′·NAD.

The NMR data indicate that when a third subunit becomes occupied, there is a stabilization of the E′·NAD complex for one subunit, for example, by a decrease in $k_{-2}$ which leads to slow-exchange conditions with $K_2 \gg 1$ and minimal exchange line width for one bound and now visible $\beta$-NAD. This behavior could be explained by a model in which an occupied subunit requires two occupied neighbors to stabilize the E to E′ transition. Occupation of the fourth subunit would then be necessary to convert at least a second subunit to E′. With full saturation of the fourth site a complete transition to holoenzyme with four equivalent E′·NAD units is expected. The proposed conformational change would result in a reduced apparent dissociation constant $K_D^{app} = K_D/(1 + K_2)$ for the E′ state. In addition, an E′ subunit may reduce the affinity of a neighboring subunit for $\beta$-NAD by a reduction in $k_1$. Such effects could explain the increase in $K_D$ reported for the third and fourth sites.

In the literature[3,11,13] one finds $K_D$ values for the first and second NAD in the range of 0.05–0.2 $\mu$M and for the third and fourth NAD in the range of 0.5–3.0 $\mu$M, depending on temperature and method of measurement and on the assumed model of negative

(14) Martin, M. L.; Martin, G. J.; Delpuech, J. J. *Practical NMR Spectroscopy*; Heyden: London, 1980; pp 293–303.

cooperativity. For our experiments the subunit concentration was ca. 600 $\mu$M. For 4 $\beta$-NAD/tetramer the percent saturation of sites can be calculated to be 96 or 88% for $K_D^{app}$ = 1 or 10 $\mu$M, respectively. For 6 $\beta$-NAD/tetramer, where we find a maximum in detectable bound $\beta$-NAD, 97% binding will be achieved for $K_D^{app}$ = 10 $\mu$M. Thus, the excess $\beta$-NAD required for complete detection of bound $\beta$-NAD is consistent with the range of $K_D$ values reported for the third and fourth sites. If we assume that the holoenzyme has all four subunits in the E′ form and that near saturation only tetramers containing three or four $\beta$-NAD molecules are present, then the following relation can be derived for the fraction $f'$ of sites that are in the detectable E′·NAD state:

$$f' = (4 - n)Y + n - 3 \quad (2)$$

where $Y$ is the fractional saturation for all subunits and $n$ = 1, 2, or 3 is the number of subunits converted into E′ in the tetramer containing three $\beta$-NAD. For $n$ = 3 we have $f' = Y$; i.e., all bound $\beta$-NAD would be detectable by NMR near a stoichiometry of 4 $\beta$-NAD/tetramer. For $n$ = 1 we have $f' = 3Y - 2$, which means that $f'$ is only 0.5 for $Y$ = 0.83. This latter case agrees with our observation that only ca. 50% of the bound $\beta$-NAD is detectable as E′·NAD for $\beta$-NAD/tetramer $\lesssim$ 4. This leads us to propose the following scheme for the major GAPDH species present during titration with $\beta$-NAD:

| | | | | |
|---|---|---|---|---|
| OO | NO | NN | N′N | N′N′ |
| OO | OO | OO | NO | N′N′ |

where O is a subunit without $\beta$-NAD, N is a subunit with "invisible" NAD, N′ is an E′·NAD subunit.

Our simple model assumes that NAD only binds and dissociates through the E state. More complicated models involving an E $\rightleftharpoons$ E′ equilibrium without NAD and direct binding of NAD to an E′ state can be envisaged. However, due to the limitations in the quality of our data and the many unknown parameters for a tetrameric enzyme with interacting subunits, we do not feel that more detailed mathematical analyses or dynamic NMR line-shape simulations are warranted at this time.

According to eq 1 the observed line width of free NAD in slow exchange with E·NAD can be expressed as[15]

$$\pi\Delta\nu_f = \pi\Delta\nu_o + k_1[E] = \pi\Delta\nu_o + k_{-1}^{app}[NAD]_{bound}/[NAD]_{free} \quad (3)$$

where $[NAD]_{bound} = [E{\cdot}NAD] + [E'{\cdot}NAD]$, $k_{-1}^{app} = k_{-1}/(1 + K_2)$, and $\Delta\nu_o$ is the line width in the absence of exchange. Thus, the slope of the straight line in Figure 6 defines the apparent dissociation rate $k_{-1}^{app}$ = 23 s$^{-1}$ at 15 °C for $\beta$-NAD from the holoenzyme. This low rate indicates that the lower affinity of GAPDH for the fourth coenzyme molecule is not likely to be a result of a higher dissociation rate but must reflect a lower effective association rate due to the requirement of promoting the E to E′ transition.

The expected line width for the C-4 signal of NAD bound rigidly to an isotropically tumbling tetramer can be estimated by inserting an appropriate correlation time $\tau_c$ and internuclear distance $r_{CH}$ into the standard equation for the relaxation time $T_2$. For MW $\sim$ 145 000 the value of $\tau_c$ is estimated to be 100 $\pm$ 20 ns at 15 °C under our conditions.[16] For an H-atom bound to an aromatic ring ($r_{CH}$ = 1.06 Å) one obtains $\Delta\nu_{calc}$ = 170 $\pm$ 30 Hz. The observed value of $\Delta\nu_b$ = 260 $\pm$ 30 Hz is somewhat larger and may contain a contribution to relaxation from protein protons packed close to C-4 in the binding site. An upper limit for the kinetic contribution to the line width is $k_{-2} < \pi(\Delta\nu_b - \Delta\nu_{calc}) \sim 300$ s$^{-1}$. For the holoenzyme $\Delta\nu_b$ decreased to 210 Hz at 23 °C as expected for a longer $T_2$ due to shorter $\tau_c$ but then increased to 300 Hz at 30 °C, indicating the onset of an increased conformational exchange rate ($k_{-2}$).

**Nature of NAD Binding.** The discussion concerning the mode of NAD binding to GAPDH began in 1952 with the discovery of the "Racker band", where upon addition of NAD to the apoenzyme an absorption band appears at 360 nm.[12] Kosower[17] suggested a charge-transfer-type complex between NAD and some residue of GAPDH, possibly Cys[149]. X-ray crystallographic data[18,19] revealed that the phenolic ring of the invariant residue Tyr[317] is approximately parallel to the pyridinium ring at a distance of ca. 4 Å and could form a charge-transfer complex with it. Recent studies with mutants have shown that Cys[149] but not His[176] or Tyr[317], which are all at the binding site, is involved in the formation of this band.[18] Two hypotheses were put forward to explain the involvement of Cys[149]: (a) covalent bonding of the cysteine sulfur to the C-4 atom of NAD[12,20] or (b) an electron donor–acceptor interaction of these two participants.[21] The first hypothesis can now be unequivocally ruled out. The downfield shift of C-4 upon binding of $\beta$-NAD clearly excludes the addition of a nucleophile at C-4, which would have a chemical shift of ca. 70 ppm, as found for our model compound **3**. Phenylthiol adducts of symmetrical N-methylated nicotinamide and analogues (substituted amide functions at positions 3 and 5) have been investigated by NMR,[20] and chemical shifts for C-4 were ca. 40–60 ppm in $CDCl_3$ and 20–30 ppm further downfield in polar solvents. This led van Keulen and Kellogg[20] to propose an equilibrium of the covalent thio adduct with an undissociated "intimate" pyridinium–thiolate ion pair (stabilized by hydrogen bonding with an amide NH) in which C-4 develops some positive charge but still retains sp$^3$ hybridization. The authors went on to speculate about the possible role of such a complex involving the active Cys[149] and bound NAD in GAPDH. However, they failed to explain why C-4 in the analogous benzylthio adducts showed no such solvent-dependent shift. During our titration of GAPDH with $\beta$-NAD we observed no additional signals at 40–90 ppm, either at partial or at full saturation with $\beta$-NAD. This rules out a covalent thio adduct as well as the localized ion pair proposed by van Keulen and Kellogg.[20]

Our model compound **3** shows that the addition of a thiol at C-4 causes the signals of all remaining sp$^2$-hybridized C-atoms of the pyridine ring to experience an upfield shift, as expected for the increased electron density in the ring. Because $^{13}$C NMR data for C-6 and C-2 adducts of $\beta$-NAD are lacking, we reduced a sample of [4-$^{13}$C]NAD with sodium borohydride, which results in the formation of a ca. 1:1:1 mixture of 1,4-, 1,6-, and 1,2-NADH.[22] The product mixture exhibited three major $^{13}$C NMR signals at 23, 121, and 136 ppm. Thus, reduction at C-2 or C-6 also leads to an upfield shift for C-4, and it therefore appears unlikely that a nucleophilic attack at C-2 or C-6 could be responsible for the ca. 6 ppm downfield shift of C-4 upon binding to GAPDH.

It is known that the C-4 chemical shift for $\beta$-NAD contains an upfield ring current shift contribution due to a folded conformation present to an extent of perhaps 30%.[23] This is reflected in the upfield shift of $\beta$-NAD vs NMN (Table I). The binding of $\beta$-NAD to GAPDH in an "open" conformation[19] is therefore expected to result in only a ca. 1 ppm downfield shift at C-4. Environmental effects due to ring currents from aromatic residues would also normally contribute only 1–2 ppm to the C-4 shift. A downfield shift would require an edge-on contact with Tyr[317], for example, but its parallel orientation to the nicotinamide ring in the crystal structure[18] would allow for only a weak upfield shift. Hydrophobic packing effects are also predicted to give small upfield shifts to carbon. The X-ray structure[19] of the holoenzyme

(15) Hull, W. E.; Halford, S. E.; Gutfreund, H.; Sykes, B. D. *Biochemistry* **1976**, *15*, 1547–1561.
(16) Sykes, B. D.; Hull, W. E.; Snyder, G. H. *Biophys. J.* **1978**, *21*, 137–146.
(17) Kosower, E. M. *J. Am. Chem. Soc.* **1956**, *78*, 3497–3501.
(18) Mougin, A.; Corbier, C.; Soukri, A.; Wonacott, A.; Branlant, C.; Branlant, G. *Protein Eng.* **1988**, *2*, 45–48.
(19) Skarzynski, T.; Moody, P. C. E.; Wonacott, A. J. *J. Mol. Biol.* **1987**, *193*, 171–187.
(20) van Keulen, B. J.; Kellogg, R. M. *J. Am. Chem. Soc.* **1984**, *106*, 6029–6037.
(21) Cseke, E.; Boross, L. *Acta Biochim. Biophys. Acad. Sci. Hung.* **1967**, *2*, 39–46.
(22) Chaykin, S.; Meissner, L. *Biochem. Biophys. Res. Commun.* **1964**, *14*, 233–240.
(23) Oppenheimer, N. J.; Arnold, L. J.; Kaplan, N. O. *Biochemistry* **1978**, *17*, 2613–2618.

Table II. Determination of the $NAD^+$ Concentration in the Individual NMR Samples by UV Measurements and Enzymic Assay

| spectrum no.[a] | ratio $E_{280}/E_{260}$ | $\epsilon$ (mL $mg^{-1}$ $cm^{-1}$)[b] | total $NAD^+$/tetramer of apoenzyme (mol/mol)[c] | $\beta$-NAD/tetramer of apoenzyme (mol/mol)[d] | $\beta$-NAD/tetramer of apoenzyme (YADH)[e] |
|---|---|---|---|---|---|
| 1.2 | 1.725 | 0.933 | 0.90 | 0.72 | 0.68 |
| 1.3 | 1.457 | 0.971 | 1.75 | 1.40 | 1.37 |
| 1.4 | 1.295 | 1.008 | 2.55 | 2.04 | 2.06 |
| 2.2 | 1.278 | 1.016 | 2.75 | 2.01 | 2.08 |
| 2.3 | 1.152 | 1.058 | 3.70 | 2.70 | 2.72 |
| 1.5 | 1.149 | 1.056 | 3.65 | 2.92 | 2.76 |
| 2.4 | 1.052 | 1.100 | 4.70 | 3.43 | 3.25 |
| 2.5 | 0.971 | 1.143 | 5.60 | 4.09 | 3.98 |
| 1.6 | 1.000 | 1.127 | 5.25 | 4.20 | 4.18 |
| 1.7 | 0.881 | 1.190 | 6.70 | 5.36 | 5.62 |
| 1.8 | 0.763 | 1.252 | 8.05 | 6.44 | 6.71 |
| 1.9 | nd[f] | nd | nd | nd | 8.14 |

[a] Contents of the coenzyme reagent as determined by NMR and HPLC: (series 1) 76.1% $\beta$-$NAD^+$/19.0% $\alpha$-$NAD^+$/4.9% $NMN^+$; (series 2) 61.0% $\beta$-$NAD^+$/22.5% $\alpha$-$NAD^+$/16.5% $NMN^+$. [b] Extinction coefficient as a function of the $NAD^+$ content of GAPDH.[3] [c] Total $NAD^+$ ($\alpha + \beta$) as determined by the UV method of Seydoux et al.[3] [d] Calculated $\beta$-$NAD^+$/tetramer = total $NAD^+$/tetramer (Seydoux) × 0.80 (series 1) or 0.73 (series 2). [e] $\beta$-$NAD^+$ alone, as determined by the yeast alcohol dehydrogenase assay.[20] [f] nd = not determined.

shows that there are probably two hydrogen bonds involving the nicotinamide amide group, which may have an inductive or resonance effect withdrawing electron density at C-4 and contributing to a downfield shift.

The unusually large shift observed is apparently associated with the occurrence of the Racker band and indicates that aromaticity of the positively charged pyridinium ring is maintained and that electron density at C-4 is further reduced. The pyridinium–thiolate ion pair model[20], in a less "intimate" form than discussed above, could provide an explanation for the C-4 shift. A partially or completely ionized thiolate could be formed from $Cys^{149}$ and stabilized by hydrogen bonding with $His^{176}$[18] or with the amide group of NAD.[20] The pyridinium cation of NAD would remain delocalized with C-4 in $sp^2$ hybridization, but a slight increase in partial positive charge at C-4 could be induced by the thiolate negative charge and be responsible for the observed downfield shift ($\delta_c = -160$ ppm per $\pi$ electron). A thiolate to pyridinium charge transfer transition for this ion pair could be the source of the Racker band. Such a model makes mechanistic sense by avoiding an unproductive covalent intermediate of the form proposed by van Keulen and Kellogg.[20] $Cys^{149}$ is activated for nucleophilic attack at the substrate aldehyde group, and an increased electron deficiency at C-4 of the bound coenzyme would facilitate hydride transfer from the substrate to C-4.

## Conclusions

The initial "NMR invisibility" of bound $\beta$-NAD in the titration of apoGAPDH can be explained by a three-site exchange model (eq 1) for each subunit, whereby a conformational equilibrium between E·NAD and E′·NAD complexes with different C-4 chemical shifts is in the coalescence regime ($\tau_{ex} \sim 1$ ms) with severe line broadening for bound $\beta$-NAD. Subunit interactions induced by the binding of the third and fourth $\beta$-NAD result in a stabilization of first one and then of all subunits in the detectable E′·NAD form, respectively. This explains the rapid increase in E′·NAD observed as sufficient excess $\beta$-NAD is added to saturate all subunits. The energy required for the E → E′ conversion is supplied at the expense of the progressively weaker binding constants reported in the literature for the third and fourth $\beta$-NAD (negative cooperativity). The low value for the apparent rate constant for dissociation of $\beta$-NAD from the holoenzyme (23 $s^{-1}$) indicates that the lower affinity of the fourth $\beta$-NAD site can best be explained by a lower effective association rate $k_1$ as a result of the conformational changes that are being driven. The unusually large downfield chemical shift of C-4 upon binding (ca. 6 ppm) rules out any type of stable complex involving a nucleophilic addition to the pyridinium ring and supports the concept of an ion pair complex, possibly involving a thiolate anion formed from $Cys^{149}$, the residue which is implicated in the Racker band.[18]

The apparent "2+2" behavior of the subunits in our experiments is noteworthy since the crystal structure[19] indicates that the subunits are arranged with 222 molecular symmetry and that pairs of coenzyme binding sites related by the $R$ axis are closer together. Our results and the model for a conformational equilibrium altered by $\beta$-NAD binding complement the previous observations of Malhotra and Bernhard[24] regarding NAD as effector for the formation and kinetics of the acyl-GAPDH. Our results provide evidence for the "induced-fit" model of cooperativity, in which an asymmetry of subunit interactions at partial saturation rather than a preexistent asymmetry of subunit conformation is required.

## Experimental Section

**Materials.** Glyceraldehyde-3-phosphate dehydrogenase from sturgeon muscle was isolated according to a published procedure.[3] The relatively stable apoenzyme exhibited a specific activity of 252 units/mg and was homogeneous by SDS–polyacrylamide gel electrophoresis.[25]

[4-$^{13}$C]Nicotinamide (99%) was synthesized by slight modification of the procedure previously described.[10] Two batches of [4-$^{13}$C]$NAD^+$ were prepared by NADase-catalyzed exchange with thio-$NAD^+$.[26] As in our previous work[10] the $^{13}$C-labeled product mixture contained both $\alpha$- and $\beta$-NAD, and the NMR experiments also detected a small amount of $NMN^+$. $\alpha$-NAD and NMN did not interact with GAPDH and were used as controls for the amount of $\beta$-NAD added. Two series of binding studies were carried out, and the contents of the coenzyme solutions are given in Table II.

**Synthesis of 3-Methyl-1-thia-4,8-diazabicyclo[5.4.0]undeca-6,9-dien-5-one (3).** Nicotinic acid (3.1 g; 25 mmol) and cystamine hydrochloride (3.38 g; 15 mmol) were heated to 40 °C in dry toluene (40 mL). To this mixture was added phosphoryl chloride (1.9 g; 1.15 mL), followed by heating to 110 °C for 14 h. After cooling to 0 °C and addition of water (15 mL), the reaction mixture was neutralized with solid sodium carbonate. The dark red aqueous phase was extracted with toluene (3 × 20 mL), and the combined organic extract was concentrated in vacuo. The product **1** (1.17 g; 3.2 mmol; yield 21.5%), a red solid, was insoluble in water but soluble in chloroform: $^1$H NMR (250 MHz, $CDCl_3$) $\delta$ 3.45 (t, $J$ = 8.4 Hz, 2 H), 4.46 (t, $J$ = 8.4 Hz, 2 H), 7.35 (dd, 1 H, H-5), 8.1 (dt, 1 H, H-4), 8.67 (dd, 1 H, H-6), 9.04 (d, 1 H, H-2); $^3J_{45}$ = 8.03 Hz, $^3J_{56}$ = 4.1 Hz.

The crude disulfide **1** (0.364 g; 1.01 mmol) was dissolved in acetone (25 mL) and treated with methyl iodide (0.16 g; 1.12 mmol) at 60 °C for 8 h. The resulting yellow precipitate **2** was filtered off and washed with acetone: yield 0.589 g (0.912 mmol; 90.3%); mp 180 °C dec; IR (KBr) 665, 689, 805, 815, 926, 985, 1000, 1028, 1067, 1090, 1130, 1152, 1205, 1265, 1295, 1320, 1430, 1460, 1492, 1550, 1575, 1590, 1630, 1650–1670, 2920, 2990, 3005–3025, 3340–3600 $cm^{-1}$; UV (MeOH) $\lambda_{max}$ 266 ($\epsilon$ 1.07 × $10^7$ $cm^2$/mol), 226 ($\epsilon$ 4.22 × $10^7$ $cm^2$/mol), 300 nm ($\epsilon$ 3.6 × $10^6$ $cm^2$/mol); $^1$H NMR (250 MHz, $D_2O$) $\delta$ 3.71 (t, $J$ = 8.2 Hz, 2 H), 4.51 (s, 3 H), 4.56 (t, $J$ = 8.2 Hz, 2 H), 8.25 (dd, 1 H, H-5), 8.88 (d, 1 H, H-4), 8.98 (d, 1 H, H-6), 9.26 (s, 1 H); $^3J_{45}$ = 8.3 Hz, $^3J_{56}$ = 6.6 Hz.

The methylated disulfide **2** (0.2 g; 0.308 mmol) and 1,4-dithioerythritol (47.6 mg; 0.308 mmol) were dissolved in water (20 mL), and a 2 M NaOH solution (2 mL) was added to the mixture, which was then

(24) Malhotra, O. P.; Berhard, S. A. *Biochemistry* **1981**, *20*, 5529–5538.
(25) Laemmli, U. K. *Nature* **1970**, *227*, 680–685.
(26) (a) Stein, A. M.; Lee, J. K.; Anderson, C. D.; Anderson, B. M. *Biochemistry* **1963**, *2*, 1015–1017. (b) Stein, A. M.; Lee, J. K.; Anderson, C. D.; Anderson, B. M. *Biochemistry* **1963**, *2*, 1017–1022.

stirred at 25 °C for 7 h under nitrogen. After evaporation of the solvent in vacuo (<30 °C), the residue was dissolved in methanol and chromatographed on preparative silica gel plates (1-propanol/10% aqueous $NH_3$, 95/5 v/v) to give the model compound **3**: yield 113.3 mg (0.57 mmol; 93.6%); MS (70 eV, $T_d$ = 100 °C) 152 (100), 194 (65), 195 (7), 196 (3) ($M^+$); UV (MeOH) $\lambda_{max}$ 270 ($\epsilon$ 5.92 × $10^6$ $cm^2$/mol), 310 nm ($\epsilon$ 3.07 × $10^6$ $cm^2$/mol); $^1H$ NMR (250 MHz, $CD_3OD$) $\delta$ 3.4 (1 H), 3.53 (t, $J$ = 8.2 Hz, 2 H), 3.65 (s, 3 H), 4.39 (t, $J$ = 8.2 Hz, 2 H), 6.6 (d, 1 H), 7.96 (dd, 1 H), 8.25 (d, 1 H); $^3J_{56}$ = 9.1 Hz, $^4J_{26}$ = 3.3 Hz; $^{13}C$ NMR (62.9 MHz, $CD_3OD$) $\delta$ 34.43 (t, $CH_2$-S), 38.39 (q, $CH_3N$), 63.85 (t, $CH_2N$), 70.09 (d, C-4), 114.29 (s, C-3), 120.1 (d, C-5), 139.66 (d, C-6), 143.44 (d, C-2), 164.75 (s, CONH), 169.43 (s).

**Preparation of Samples for NMR Measurements.** Two series of experiments for the NAD binding studies were carried out with slightly different enzyme concentrations. In the following, data for series 2 are in parentheses. To 45.12 (32.69) mg of GAPDH in 1.6 mL of buffer solution (1 mM potassium phosphate, pH 7.0, 0.5 mM EDTA, and 0.5 mM dithiothreitol) was added 0.2 mL of $^2H_2O$, resulting in a final concentration of 0.174 (0.126) mM for the tetrameric enzyme.

The [4-$^{13}$C]NAD solutions used in the two series of experiments also differed slightly (see Table II). The two solutions contained 2.41 (1.05) mg of $\beta$-NAD in 0.173 (0.100) mL of the above buffer. Introduction of a 10-$\mu$L aliquot of this coenzyme solution into the enzyme sample resulted in the addition of 0.68 (0.70) equiv of $\beta$-NAD to the tetrameric GAPDH.

**Determination of Enzyme and Coenzyme Concentrations.** Since NMR monitoring of the binding of $\beta$-NAD to GAPDH disclosed unexpected behavior, precise determination of concentrations was required. The enzyme concentration was determined by enzymic assay[27] on the one hand and by measuring the protein concentration on the other. The latter was determined by the Warburg method, which was specially adapted for GAPDH by Seydoux et al.[3] Protein determinations at the Karlsruhe and Strasbourg laboratories using this method did not differ by more than 2%. Two different methods were also applied for the determination of coenzyme concentrations, and after correction for the amounts of $\alpha$-NAD and NMN present, they gave consistent results. The percentages of the different nicotinamide nucleotide species in the coenzyme samples were determined by $^{13}$C NMR and independently by HPLC.[28]

After each addition of [4-$^{13}$C]NAD a 20-$\mu$L aliquot of the mixture was withdrawn, and its NAD content was determined according to the method of Seydoux et al.[3] Since this method relies on the UV absorption at 260 nm, the determination also includes unbound $\alpha$-NAD. Taking this into account, the calculated $\beta$-NAD values showed good agreement with those determined independently by the yeast alcohol dehydrogenase reaction (Table II).[29] Variations of the enzyme concentration in the reaction mixture caused by withdrawal and/or addition of aliquots are also accounted for in the tables.

**$^{13}$C NMR Spectroscopy.** $^{13}$C NMR spectra of the enzyme/coenzyme mixtures were obtained at 125.7 MHz (11.7 T) on a Bruker AM-500 FT-NMR spectrometer. The ca. 1.8-mL samples were measured at a controlled temperature of 15 °C in 10-mm sample tubes (nonspinning without a vortex plug to avoid a Teflon background signal). Chemical shifts were referenced to internal dioxane ($\delta_c$ = 67.8 ppm) by use of a separate buffer solution. All measurements were performed with the standard inverse-gated decoupling technique to obtain $^1$H-decoupled spectra with suppression of the nuclear Overhauser effect (NOE) in order to ensure that signal integrals were proportional to concentrations for all species. Parameters for data acquisition were spectral width = 33 kHz for 16K time domain points with an acquisition time of 0.246 s and pulse width = 15 $\mu$s (flip angle ca. 60°). The relaxation delay with the decoupler turned off was 0.6 s for spectra 1.1-1.7 of series 1 and 1.6 s for spectra 1.7b, 1.8, and 1.9 and spectra of series 2. Comparing spectra 1.7 and 1.7b acquired for the same sample showed that a relaxation delay of 0.6 instead of 1.6 s led to an increase in the integrals for the nonbinding species $\alpha$-NAD and NMN (partial NOE) but had no effect on bound or free $\beta$-NAD. Increasing the delay to 2.3 s (spectrum 1.9b) caused no further change in any signal intensities. Therefore, the spectra of series 2 were all obtained with the 1.6-s delay. For spectra 1.1-1.7 the integrals measured for $\alpha$-NAD and NMN were corrected for the observed effect of the shorter delay. The number of transients acquired for each spectrum ranged from 4000 (spectra 1.8 and 1.9 in 2 h) to 40 000 (spectrum 2.5 in 20 h).

Spectra were Fourier transformed with 32K data points (a) after an exponential multiplication with 30-Hz line broadening for quantitative analysis of total free and total bound species (Figure 2) and (b) with a Lorentz-Gauss resolution enhancement (Bruker software; LB = -8; GB = 0.1) for separate integration and line-width evaluation of the resolved signals for free $\beta$-NAD, $\alpha$-NAD, and NMN (Figures 3 and 6). Transforms were in absolute-intensity mode referenced to spectrum 1.7b, and integrals were then appropriately scaled according to the different number of transients acquired for each spectrum to give the data of Table I and Figure 4. The integrals from the spectra of series 2 were also corrected by a scaling factor which took into account the lower initial enzyme concentration compared to that in series 1. The scaling factors used were also applied to the spectra themselves to produce the figures. Subtraction of spectrum 1.7 or 1.7b from individual scaled spectra obtained with the same relaxation delay showed that the theoretical scaling factors agreed with empirical scaling factors within ca. 5%, as judged by cancellation of the lysine signal of GAPDH at ca. 40 ppm. Integration of the base line corrected spectra was performed digitally with the standard routines of the Bruker NMR software.

**Acknowledgment.** We thank P. Barth for help in the enzyme purification and the Deutsche Forschungsgemeinschaft and the Fonds der Chemischen Industrie for financial support. J.K. thanks the province of Baden-Württemberg for a scholarship.

(27) Ferdinand, W. *Biochem. J.* **1964**, *92*, 578-585.
(28) Richard, A. H.; Sebastian, P. A.; Phyllis, R. B. *J. Chromatogr.* **1979**, *186*, 647-658.
(29) Lowry, O. H.; Passonneau, J. V. *A Flexible System of Enzymatic Analysis*; Academic Press: New York, 1972.

# Hydrolysis of *N*-Acetyl-*p*-benzoquinone Imines: pH Dependence of the Partitioning of a Tetrahedral Intermediate

**Michael Novak,* Gayl A. Bonham, Julio J. Mulero,[1a] Maria Pelecanou,[1a] Joseph N. Zemis,[1a] Jeanne M. Buccigross,[1b] and Thomas C. Wilson**

*Contribution from the Department of Chemistry, Miami University, Oxford, Ohio 45056.*
*Received November 17, 1988*

**Abstract:** The hydrolysis reactions of *N*-acetyl-*p*-benzoquinone imine, **1a**, and its 3,5- and 2,6-dimethyl analogues, **1b** and **1c**, in the pH range 0.3-10.5 are described. At pH < 6.0 the carbinolamide intermediates **2a-c** can be detected by $^1$H NMR, UV, and HPLC methods. The pH-dependent partitioning of **2a** and **2c** can be monitored since the reversion of these intermediates to the protonated *N*-acylimines **5a** and **5c** leads to products of the conjugate attack of $Cl^-$, the 3-chloroacetaminophen derivatives **4a** and **4c**. A mechanism for the hydrolysis of **1a-c** (Scheme I) is proposed which accurately predicts the time dependence of the formation of **2** and the final hydrolysis products, the *p*-benzoquinones **3**, and **4**. The alternative O-protonation mechanism (Scheme II) is tentatively rejected on the basis of substituent effect data. The relationship of the hydrolysis reactions of **1a-c** to those of ordinary imines is discussed.

*N*-Acetyl-*p*-benzoquinone imine (**1a**) is an apparent toxic metabolite of the common analgesics acetaminophen and phenacetin.[2] The mechanism of action of **1** in vivo is not well understood, and little is known of its aqueous-solution chemistry.

0002-7863/89/1511-4447$01.50/0 